Role of small Rhizaria and diatoms in the pelagic silica production of the Southern Ocean

Natalia Llopis Monferrer, Aude Leynaert, Paul Tréguer, Andrés Gutiérrez-Rodríguez, Mikel Latasa, Karl Safi, Matthew H Pinkerton, Brivaëla Moriceau, Stéphane L'Helguen, Jean-François Maguer, et al.

LIMNOLOGY and OCEANOGRAPHY

ASLO

Limnol. Oceanogr. 9999, 2021, 1–16

doi: 10.1002/lno.11743

Role of small Rhizaria and diatoms in the pelagic silica production of the Southern Ocean

Natalia Llopis Monferrer,[1,2*] Aude Leynaert,[1] Paul Tréguer,[1] Andrés Gutiérrez-Rodríguez,[3] Brivaela Moriceau,[1] Morgane Gallinari,[1] Mikel Latasa,[4] Stéphane L'Helguen,[1] Jean-François Maguer,[1] Karl Safi,[5] Matthew H. Pinkerton,[3] Fabrice Not[2]

[1]Univ Brest, CNRS, IRD, Ifremer, LEMAR, F-29280, Plouzane, France
[2]Sorbonne University, CNRS, UMR7144, Ecology of Marine Plankton Team, Station Biologique de Roscoff, Roscoff, France
[3]National Institute of Water and Atmospheric Research, Wellington, New Zealand
[4]Centro Oceanográfico de Gijón/Xixón, Instituto Español de Oceanografía (IEO), Gijón/Xixón, Asturias, Spain
[5]National Institute of Water and Atmospheric Research, Hamilton, New Zealand

We examined biogenic silica production and elementary composition (biogenic Si, particulate organic carbon and particulate organic nitrogen) of Rhizaria and diatoms in the upper 200 m along a transect in the Southwest Pacific sector of the Southern Ocean during austral summer (January–February 2019). From incubations using the ^{32}Si radioisotope, silicic acid uptake rates were measured at 15 stations distributed in the Polar Front Zone, the Southern Antarctic Circumpolar Current and the Ross Sea Gyre. Rhizaria cells are heavily silicified (up to 7.6 nmol Si cell^{-1}), displaying higher biogenic Si content than similar size specimens found in other areas of the global ocean, suggesting a higher degree of silicification of these organisms in the silicic acid rich Southern Ocean. Despite their high biogenic Si and carbon content, the Si/C molar ratio (average of 0.05 ± 0.03) is quite low compared to that of diatoms and relatively constant regardless of the environmental conditions. The direct measurements of Rhizaria's biogenic Si production (0.8–36.8 μmol Si m^{-2} d^{-1}) are of the same order of magnitude than previous indirect estimations, confirming the importance of the Southern Ocean for the global Rhizaria silica production. However, diatoms largely dominated the biogenic Si standing stock and production of the euphotic layer, with low rhizarians' abundances and biogenic Si production (no more than 1%). In this manuscript, we discuss the Antarctic paradox of Rhizaria, that is, the potential high accumulation rates of biogenic Si due to Rhizaria in siliceous sediments despite their low production rates in surface waters.

Introduction

Up to 23.5% of the overall biogenic silica production occurs within polar oceans (Tréguer and De La Rocha 2013; Tréguer 2014; Tréguer et al. 2021), most of it in the Southern Ocean. The Southern Ocean, sometimes referred to as the "silica ocean" (Honjo et al. 2008), has among the highest oceanic silicic acid concentrations. Diatoms are the major contributors to biogenic Si production in the surface Southern Ocean (e.g., Nelson and Gordon 1982; Tréguer 2014). This siliceous phytoplankton taxon often dominates microalgal assemblages in the Southern Ocean, and it is considered key in the austral food web, being responsible for up to 75% of annual primary production (Tréguer et al. 1995). Since diatoms are the dominant silicifiers, most of the studies regarding the processes that biologically control the marine Si cycle have been focused on these microalgae. However, recent studies have elevated the importance of other silicified planktonic organisms in the marine Si cycle. Silicified polycystine Radiolaria (e.g., Nassellaria, Spumellaria) and Phaeodaria, which are heterotrophic planktonic protists belonging to the Rhizaria lineage, are capable of consuming silicic acid and could contribute from 1% to 19% to the biogenic Si production of the global ocean (Llopis Monferrer et al. 2020). Unlike diatoms, that only develop in the euphotic layer, Rhizaria thrive throughout the entire water column, from surface waters to the mesopelagic and bathypelagic ocean (Suzuki and Not 2015).

Despite evidence of the presence of these organisms in the Southern Ocean and the importance of this region in the oceanic Si cycle (Tréguer 2014), to our knowledge the contribution of Rhizaria to the biogenic Si production in the surface layer of the Southern Ocean has never been assessed. Some

*Correspondence: natalia.llopismon@univ-brest.fr

studies have reported the presence of Rhizaria in the Southern Ocean water column (Nöthig and Gowing 1991; Klaas 2001), and numerous sedimentary records document their abundances in polar regions (Dutkiewicz et al. 2015; Maldonado et al. 2019). The sedimentation and accumulation of silicifiers in the Southern Ocean creates a prominent siliceous-rich deposit on the seabed around the globe, with a northern limit at the Polar Front Zone. This deposit, also known as the Antarctic opal-belt (Tréguer et al. 1995), is mainly composed by diatomaceous oozes, but can also contain abundant skeletons of siliceous radiolarians (Dutkiewicz et al. 2015; Maldonado et al. 2019). In order to contribute to the understanding of Si biogeochemical cycle and better constrain the contribution of Rhizaria to the Si cycle in the Southern Ocean, this regional study specifically aims to (i) determine the abundance, biomass and elemental composition of siliceous Rhizaria and diatoms, and (ii) measure the Si uptake rates, in the upper water column (0–200 m) of the southwest Pacific sector of the Southern Ocean and the Ross Sea region.

Material and methods

Study area

The *Ross Sea Marine Environment and Ecosystem Voyage 2019* (TAN1901) was conducted during austral summer (January and February 2019) on board the R/V Tangaroa, sailing from New Zealand to the Ross Sea. The survey covered mainly oceanic and shelf-slope waters of the Ross Sea region with a focus on the eastern flank of the Iselin Bank and the Ross Gyre. This study presents results from a subset of 15 stations where Conductivity, Temperature, Depth (CTD) casts and net tows were combined to assess water column biogeochemistry and where

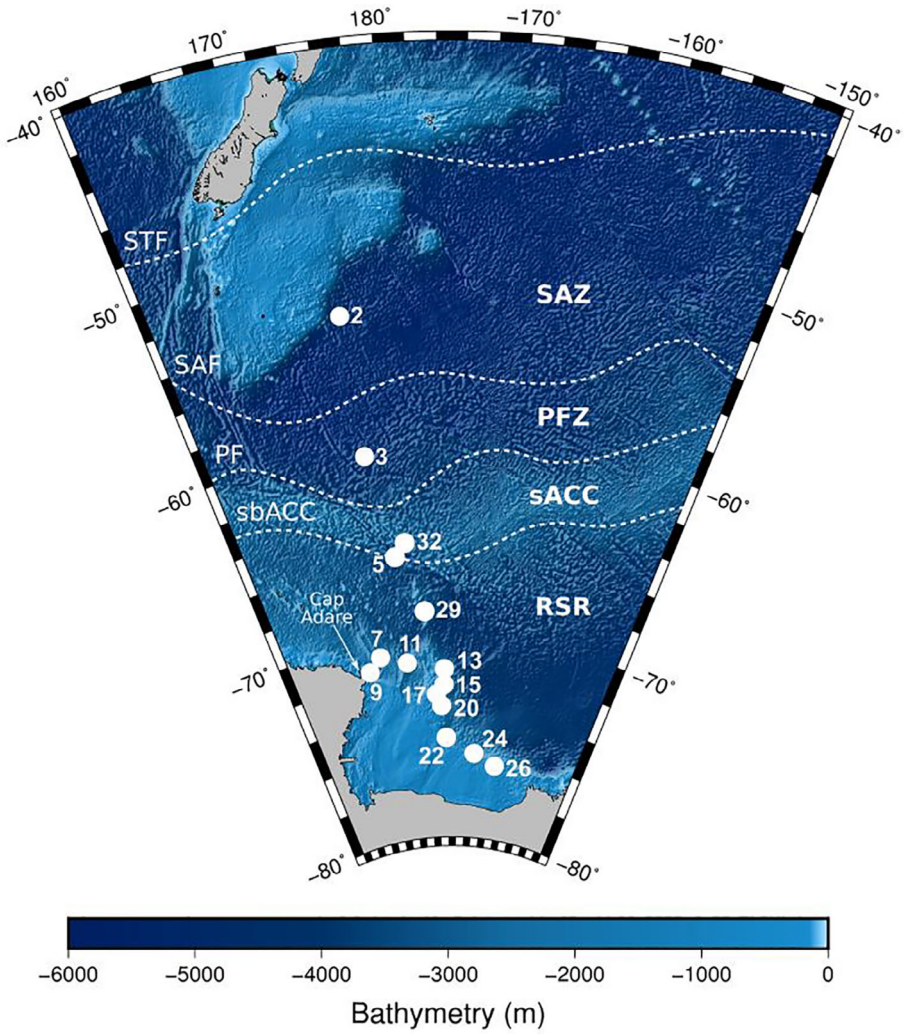

Fig 1. Map of the Southwest Pacific sector of the Southern Ocean with station locations (white dots) and approximate delineations of oceanic fronts established during the expedition. The subtropical front (STF), sub-Antarctic zone (SAZ), sub-Antarctic front (SAF), Polar Front (PF), Polar Front Zone (PFZ), Southern Antarctic Circumpolar Current (sACC), southern boundary of the ACC (sbACC), and Ross Sea Region (RSR).

silicic acid uptake rates were measured using 24-h incubation experiments.

The area studied was divided into three main hydrographically and ecologically distinct subregions arranged as zonal bands delimited by fronts (Fig. 1).

1. The Polar Front Zone: This zone is delimited by the sub-Antarctic front and the Polar Front. Only Sta. 3 was located in this subregion.
2. The Southern Antarctic Circumpolar Current: This zone is located between the Polar Front (~ 61.5°S) in the north and the southern boundary of the Antarctic Circumpolar Current in the south (~65°S). Stas. 5 and 32 were located within this subregion.
3. The Ross Sea Region: This zone lies south of the southern boundary of the Antarctic Circumpolar Current. Most of the stations were located in this zone (Stas. 7, 9, 11, 13, 15, 17, 20, 22, 24, 26, and 29).

Sta. 2 was located in the sub-Antarctic Zone, north of the three regions considered above. At this station, sampling for nutrient and biogenic silica but no plankton nets were carried out.

Sample collection and analyses

Water column: Niskin bottle samples

Dissolved material. A Seabird system was deployed to perform CTD profiles coupled with 10-liter Niskin bottles for collection of water samples from 3 to 8 discrete depths. For nutrients concentration analyses (nitrate, silicic acid), seawater was filtered by gravity into a 50-mL falcon tube using a 0.2-μm Supor filter cartridge (Acropak, Pall-Gelman) connected directly to the Niskin bottle. Samples were capped with parafilm and frozen at −20°C until analysis in the laboratory. Nutrients concentrations were measured using an Astoria Pacific API 300 micro-segmented flow analyzer (Astoria-Pacific, Clackamas, Oregon).

Particulate organic material. For the determination of particulate organic matter in the water column, seawater samples were collected in 15 stations at 6 depths between 0 and 100 m. One liter of seawater was filtered onto 0.6 μm, 47-mm isopore polycarbonate filters (GE Healthcare Whatman) for biogenic silica and lithogenic silica analyses. After filtration, filters were kept in petri dishes and stored at room temperature. Analyses were performed using the double digestion method according to Ragueneau and Tréguer (1994). After NaOH extraction, filters were analyzed for lithogenic Si by HF digestion during 48 h.

For particulate organic carbon (POC) and particulate organic nitrogen (PON) measurements, 1 liter of seawater was filtered onto 25-mm GF/F precombusted filters (at 450°C during 4 h). Filters were then dried in the oven at 60°C and kept at room temperature. Concentrations of POC and PON were measured using a C/N analyzer (Flash EA, ThermoFisher Scientific). Blanks were subtracted from each POC and PON concentration values.

Pigments. For high-performance liquid chromatography (HPLC) analysis, 2.2 liters of seawater were filtered onto 25-mm GF/F (Whatman) filters. Filters were folded and dry-blotted before storing them at −80°C until laboratory analysis. For Sta. 24, only 1.6 liters were filtered before the filter clogged. Pigments were extracted with 2.5 mL of 90% acetone spiked with 8′-apo-carotenal as internal standard. Filters in acetone were sonicated for 30 s in a tube inside a beaker with ice and stored at −20°C for 24 h. Samples were filtered prior to injection onto an 1100 Agilent HPLC system. The chromatographic conditions for the analysis are described in Latasa (2014). Standards from VKI and Sigma were used to identify and quantify pigment concentrations. We used the coefficients of Uitz et al. (2006) to make an estimation of the contribution of different phytoplankton groups to the total chlorophyll *a* (Chl *a*).

Silicic acid uptake rate. Biogenic silica production was determined as silicic acid uptake rates (ρ_P) at 3 depths for 15 stations using the radioactive isotope labeling ^{32}Si method (Tréguer et al. 1991; Leynaert et al. 1996). Polycarbonate bottles filled with 160 mL seawater were spiked with 800 Bq of radio-labeled ^{32}Si silicic acid solution (Los Alamos Laboratory, specific activity of 18.5 kBq μg Si^{-1}). Samples were immediately placed in temperature-controlled (ir33+, CAREL) deckboard incubators fitted with neutral density filters to simulate light levels corresponding to different percentages of incident irradiance (%E_0 = 70%, 40%, 28%, 16%, 4%, 1%). Flow-through incubators were placed in three high-density polyethylene (HDPE)-insulated water baths (1000 LT series), each connected independently to a closed system that regulated the temperature of the large water and the flow-through incubators inside. Bottles for silicic acid uptake rates measurements were incubated for 24 h. At the end of the incubation period, samples were filtered by gentle (< 150 mmHg) vacuum filtration onto 47-mm diameter, 0.6-μm pore-size polycarbonate membrane filters (Nucleopore) and rinsed twice with filtered seawater to wash away nonparticulate ^{32}Si. Filters for silicic acid uptake rates determination were placed in 20-mL polypropylene liquid scintillation vials loosely capped to allow the sample to dry at room temperature for 48 h. The vials were then capped tightly and stored until analysis. Activity of ^{32}Si was measured after 3 months on a scintillation counter (Tri-Carb 4910TR, Perkin Elmer) by Cerenkov method (Tréguer et al. 1991). The background for ^{32}Si radioactive activity counting was 8 counts per minute (cpm). Samples for which the measured activity was less than 3 times the background were considered to show no Si uptake and therefore not considered in further calculations. We assume that the silicic acid uptake rates were mainly due to diatoms.

Phytoplankton taxonomic identification. At each station, 500 mL samples were collected at 10 m from the Niskin bottles, and preserved in Lugol's iodine solution (1% final concentration) for enumeration and taxonomic identification of phytoplankton by inverted light microscopy according to the method of (Utermöhl 1958) and procedures described in Safi et al. (2007). Briefly, 150 mL subsamples were settled for 24 h before being examined in Utermöhl chambers on an inverted microscope (Leitz). When possible, organisms were identified to genus or species level. Biovolume was then calculated by optical microscopy for each species, by measuring between 10 and 20 cells. Phytoplankton biovolume was calculated from the dimensions of each taxon and approximated geometric shapes (spheres, cones, ellipsoids) following Sun and Liu (2003) and Olenina et al. (2006).

Net tow samples

Vertical plankton tow samples were carried out with a Bongo net (64 and 200 μm mesh size, mouth diameter: 50 cm) from 200 m to the surface every other day during the TAN1901 cruise. The volume of seawater filtered through the net was estimated using a digital flowmeter (Model 23.090-23.091—KC Denmark A/S) mounted in the mouth of the net.

Cell counting. The net tow samples were split using the Motoda box. A subsample was fixed with Lugol's iodine solution (2% final concentration). Rhizaria abundances were determined in triplicate 3 mL additional subsamples using an inverted light microscope (Zeiss Axio Vert. A1) back in the laboratory. Concentrations were estimated taking into account the volume of seawater filtrated by the net. The remaining subsample was immediately diluted in filtered seawater (FSW; 0.2 μm) and screened under the microscope to isolate single cells of siliceous Rhizaria. As the isolation process could take several hours, the samples were kept in a light- and temperature-controlled incubator (MIR-254 Cooled Incubator, Sanyo) to minimize stress to the organisms. Single-cell organisms were isolated using a Pasteur pipette and sorted according to two taxonomic groups, polycystine Nassellaria and Phaeodaria. Among the Phaeodaria, we were able to confidently differentiate two species, *Protocystis tridens* and *Protocystis harstoni*. Every specimen collected was imaged and analyzed using the ImageJ software to determine morphometric dimensions.

Particulate organic material. For POC and PON cells content of Rhizaria, from 1 to 50 individuals of the same taxonomic group and similar size were rinsed in FSW passed onto 25-mm GF/F precombusted filters (at 450°C for 4 h). Filters were dried in the oven at 60°C and kept at room temperature. Concentrations of POC and PON were measured in the laboratory using a C/N analyzer (Flash EA, ThermoFisher Scientific).

Biogenic silica and silicic acid uptake rate. For ^{32}Si incubations, 1–50 individual cells of the same taxonomic group and similar size were transferred to 20-mL glass vials filled with FSW collected at 200 m depth. Samples were then spiked with 800 Bq of the radio-labeled ^{32}Si silicic acid solution (Los Alamos Laboratory, specific activity of 18.5 kBq μg Si^{-1}). Immediately after the addition of the isotope, Rhizaria samples were placed in the deck incubators together with the water column samples. Following the 24-h incubation, the bottles' contents were filtered and processed using the same protocol as for the water column samples.

The radioactivity was measured by the Cerenkov effect (Tréguer et al. 1991) on the filters without addition of any scintillation cocktail. The Cerenkov method is less sensitive than some others (Brzezinski and Phillips 1997); however, it allows to use the materials for further biomass analyses. Results were normalized by cell abundance for cell-specific silica production. After measuring the silicic acid uptake rates, the filter was analyzed to obtain the biogenic Si of Rhizaria. A single digestion in hydrofluoric acid (HF) was performed as no interference from lithogenic Si was to be expected, since the samples only contained isolated rhizarians. We added 0.2 mL of HF 2.5 N to the polymethylpentene tubes containing the filters. The filter was then compressed and submerged in HF until air bubbles were removed. The tube was tightly capped and kept under a fume hood, at room temperature for 48 h to complete the digestion of the Rhizaria skeleton. After complete digestion, 9.8 mL of saturated boric acid solution (H_3BO_3) were added and silicic acid was measured by colorimetry on a AA3 HR Auto-Analyzer SEAL-BRAN + LUEBBE (Brzezinski and Nelson 1989). Standards used for calibration were prepared with the same matrix as for the samples (HF/H_3BO_3).

Results

Physical and chemical parameters distribution

Sea surface water temperature varied from about 10°C in the sub-Antarctic Zone to −1.5°C in the Ross Sea Region during the expedition (Fig. 2). Overall, the silicic acid concentration at 10 m depth increased along a north-to-south gradient. Surface silicic acid concentrations were lower than 1 μM Si in the sub-Antarctic Zone and in the Polar Front Zone. South of the Antarctic Circumpolar Current, concentrations of silicic acid increased to 40 μM Si (Stas. 5 and 32), reaching $\sim$ 80 μM Si (Sta. 29) within the Ross Sea Region. In contrast, nitrate surface concentrations varied only slightly compared to those of the silicic acid (mean 27 ± 4 μM N; range = 14–32 μM N). This distribution of surface nutrient concentrations shows a transition from nitrate rich but silicic acid depleted waters in the north to waters enriched with both silicic acid and nitrate at higher latitude (> 65°S), and corresponds to a sharp increase in the Si/N ratio (mol/mol) southward (Fig. 2).

Biogenic silica concentrations at 10 m depth in the water column, ranged from 0.18 μmol Si L^{-1} in the Ross Sea Region and

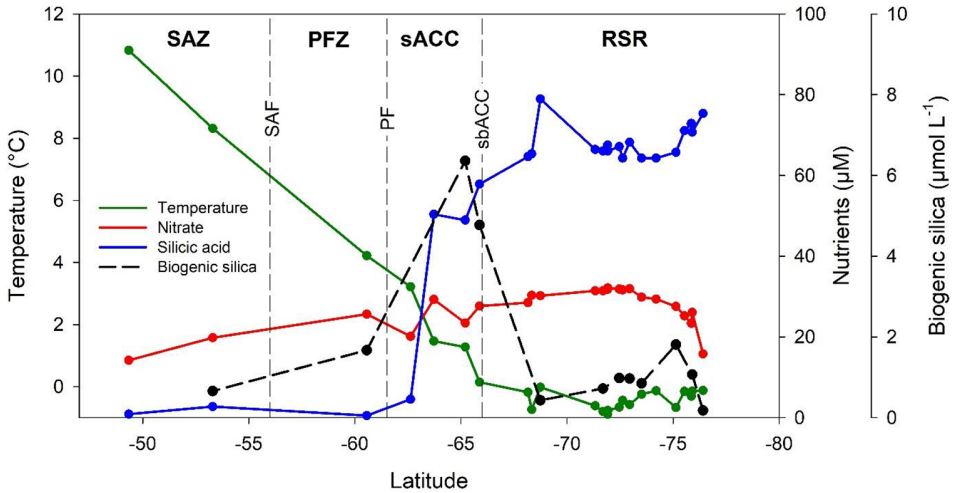

Fig 2. Distribution of temperature (green) in °C, nitrate (red), silicic acid (blue) in μM and biogenic silica (dashed-black) in μmol Si L^{-1} at 10 m depth along the cruise track from North (SW Pacific sector) to South (Ross Sea Region). Dots represent stations location. Vertical dashed lines represent the sub-Antarctic Front (SAF), the Polar Front (PF) and the southern boundary of the ACC (sbACC) delineating the four sub-regions considered for the study: the sub-Antarctic Zone, (SAZ), the Polar Front Zone (PFZ), southern ACC (sACC) and the Ross Sea Region (RSR).

Table 1. Particulate organic carbon (POC), particulate organic nitrogen (PON), and biogenic silica (bSi) concentrations. C/N and Si/C molar ratios, silicic acid uptake rates (ρ_P), and specific uptake rates (V_P) of the phytoplankton community at 10 m depth. NA means that no values were available.

Station #	Subregion	Latitude	Longitude	POC (μmol L^{-1})	PON (μmol L^{-1})	bSi (μ mol L^{-1})	C/N	Si/C	ρ_P (μmol Si d^{-1})	V_P (d^{-1})	Diatoms cell (L^{-1})
2	SAZ	−53.30	175.48	6.58	0.95	0.66	6.95	0.10	0.02	0.03	NA
3	PFZ	−60.58	175.87	7.64	1.12	1.67	6.83	0.22	0.02	0.01	NA
5	sACC	−65.86	177.94	15.39	2.46	4.77	6.26	0.31	0.25	0.05	262,544
32	sACC	−65.21	179.24	13.40	2.20	6.36	6.09	0.48	0.03	0.00	NA
Mean sACC				14.39	2.33	5.57	6.18	0.39	0.14	0.03	
7	RSR	−70.84	173.89	6.68	1.02	1.53	6.57	0.23	0.10	0.06	26,015
9	RSR	−71.50	171.95	12.08	1.92	5.47	6.28	0.45	0.34	0.06	22,079
11	RSR	−71.30	177.93	5.43	0.83	1.59	6.51	0.29	0.08	0.05	16,484
13	RSR	−71.69	−176.21	3.95	0.62	0.72	6.34	0.18	0.04	0.05	1920
15	RSR	−72.46	−176.32	6.11	1.07	0.98	5.70	0.16	0.07	0.08	30,113
17	RSR	−72.95	−177.65	6.95	1.15	0.97	6.03	0.14	0.09	0.09	103,300
20	RSR	−73.52	−176.88	5.28	0.88	0.85	6.01	0.16	0.04	0.04	9501
22	RSR	−75.13	−176.04	9.00	1.42	1.81	6.34	0.20	0.19	0.10	3800
24	RSR	−75.90	−170.56	5.65	0.92	1.07	6.14	0.19	0.10	0.09	5621
26	RSR	−76.41	−166.12	8.82	1.56	0.18	5.65	0.02	0.02	0.12	NA
29	RSR	−68.75	−178.85	6.24	1.07	0.43	5.86	0.07	0.05	0.11	NA
Mean RSR				6.93	1.13	1.42	6.13	0.19	0.10	0.08	

PFZ, Polar Front Zone; RSR, Ross Sea Region; sACC, Southern Antarctic Circumpolar Current; SAZ, sub-Antarctic Zone.

6.36 μmol Si L^{-1} in the Southern Antarctic Circumpolar Current (Table 1). With the exception of Sta. 9 (5.47 μmol Si L^{-1}), biogenic Si concentrations in the Ross Sea Region (1.42 ± 1.43 μmol Si L^{-1}, n = 11) were on average lower than in the Southern Antarctic Circumpolar Current (5.57 ± 1.12 μmol Si L^{-1}, n = 2).

Concentrations of POC at 10 m varied from 4.0 to 15.4 μmol C L^{-1} along the cruise track. Maximum concentrations were observed in the Southern Antarctic Circumpolar Current, with 15.4 μmol C L^{-1} at Stas. 5 and 13.4 μmol C L^{-1} at Sta. 32 (Table 1). Secondary peaks of POC were observed at

the southernmost station in the Ross Sea Region (Sta. 26, with 8.8 μmol C L^{-1}) and at the westernmost station (Sta. 9, with 12.1 μmol C L^{-1}), the latter being the closest to the continental shelf. The highest concentrations of PON were observed in the southern Antarctic Circumpolar Current, being on average twofold higher than the concentration measured in the Ross Sea Region (1.1 ± 0.4 μmol N L^{-1}, Table 1). Molar C/N ratios at 10 m did not vary substantially along the transect, with a minimum of 5.7 at Sta. 26 located near a polynya, and a maximum of 7.0 at Sta. 2, located in sub-Antarctic waters (Table 1), within the range observed for actively growing phytoplankton assemblages (Garcia et al. 2018).

The Si/C molar ratios of the phytoplankton community were generally high (Table 1), when compared to the reference ratio of 0.13 reported for marine diatoms (Brzezinski 1985). They averaged 0.39 in the Southern Antarctic Circumpolar Current and decreased to 0.19 in the Ross Sea Region, suggesting either a lower contribution of diatoms to the phytoplankton biomass in this area, or occurrence of more silicified diatoms in the Southern Antarctic Circumpolar Current. When integrated for the upper water column (100 m for phytoplankton community and 200 m for rhizarians due to the net tow extension), biogenic Si and POC concentrations followed a similar pattern along the transect (Fig. 3). However, there was a sharper decrease in concentration for biogenic Si than for POC within the Ross Sea Region. Highest depth-integrated concentrations for the phytoplankton community were found in the Polar Front Zone at Sta. 32, with 348.3 mmol Si m^{-2} and 1309.9 mmol C m^{-2}.

Chlorophyll a concentration and phytoplankton community composition

Surface Chl *a* concentration ranged from 101.1 to 924.3 ng Chl *a* L^{-1} (Fig. 4). The highest values observed were

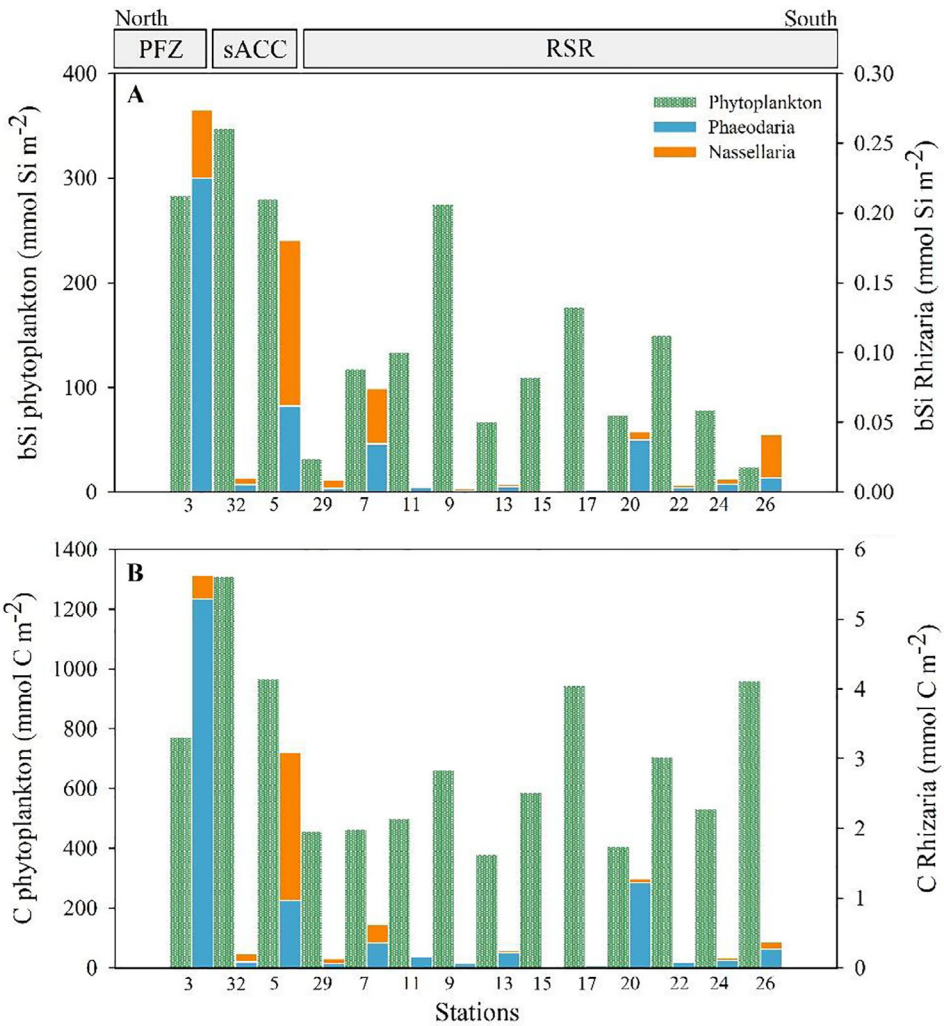

Fig 3. Biogenic silica (bSi) in mmol Si m^{-2} (**A**), and carbon in mmol C m^{-2} (**B**), of the phytoplankton community and Rhizaria integrated in the upper water column. Polar Front Zone (PFZ), southern Antarctic Circumpolar Current (sACC), and Ross Sea Region (RSR). *Y*-axis for phytoplankton and Rhizaria vary by several orders of magnitude.

associated to the Antarctic Circumpolar Current (Sta. 5) and coastal waters close to Cape Adare in the Ross Sea Region (Sta. 9). Diatoms dominated the phytoplankton community in the surface waters, accounting at least for 50% of the total Chl *a* biomass, except at Stas 26 and 3 (Fig. 4). Microscopic analyses of phytoplankton composition indicated that Sta. 17 was dominated (> 50% of abundance) by *Chaetoceros* sp. and Stas. 11 and 13 by *Corethron* sp. In the southernmost stations, we observed a dominance of the *Nitzschia* sp.

Haptophytes were the second most important taxonomic group, contributing ~ 30% of the total Chl *a* biomass, except for Sta. 26 where they accounted for > 90% of total Chl *a* (Fig. 4). Other phytoplankton groups such as dinoflagellates and green algae made up < 5% of the total Chl *a*, while the contribution of cryptophytes, pelagophytes, and *Synechococcus* was relatively minor (< 1% of the total Chl *a*).

Rhizaria cell abundances and biomass

Rhizaria abundances varied erratically between stations and ranged from < 1 to 505 cells m^{-3}, in the 0–200-m surface layer (Table 2). The highest abundances of Rhizaria (> 200 cells m^{-3}) were located at stations north of the Ross Sea Region (Stas. 3 and 5). However, Sta. 32, which was located near Sta. 5, sampled about a month later, yielded less than 30 cells m^{-3}. The lowest abundances (less than 50 cells m^{-3}) were observed within the Ross Sea Region, except at Sta. 20 where Rhizaria cells abundance reached a maximum of 111 cells m^{-3}.

Rhizaria taxonomic composition changed with latitude: in the northern sector (Polar Front Zone, Sta. 3) phaeodarians of the genus *Protocystis* dominated, whereas Nassellaria was the most abundant group in the Southern Antarctic Circumpolar Current. Among the genus *Protocystis*, *P. tridens* and *P. harstoni* were the most common species (Fig. 5). Other species such as *Protocystis swirei*, *Protocystis balfouri*, and *Protocystis micropelecus* were also recorded occasionally, but they were not abundant enough to be included in our experiments. Only taxa with sufficiently high abundance (> 30 specimens per sample) were used for the experiments. Nassellaria were largely dominated by the genus *Antarctissa* spp. (family Plagoniidae). As for Phaeodaria, the diversity of Nassellaria was noticeably higher at the northern stations, where representatives of the families Artrostrobiidae, Spyridae, and Theopteridae were common.

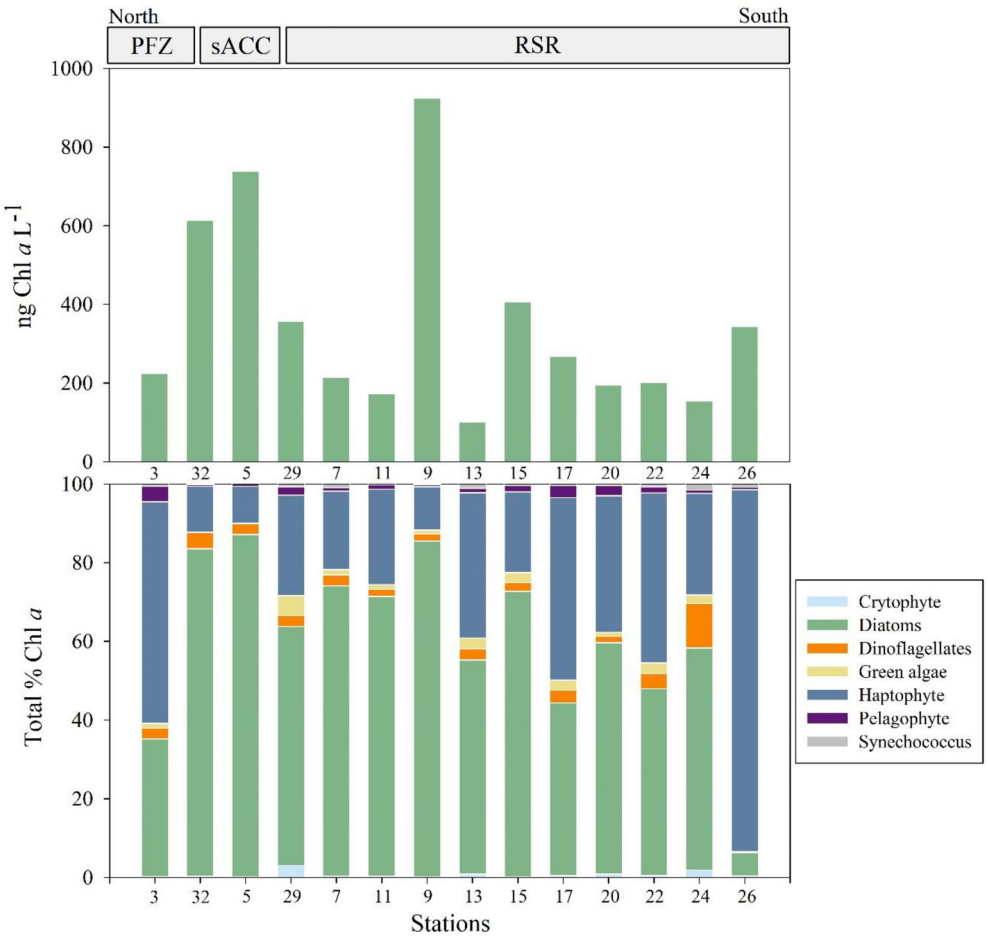

Fig 4. (**A**) Phytoplankton Chl *a* concentration in ng Chl *a* L^{-1} from north to south at the different stations. (**B**) Relative contribution of the different groups to the entire phytoplankton community. Polar Front Zone (PFZ), Southern Antarctic Circumpolar Current (sACC), and Ross Sea Region (RSR).

Table 2. Cell abundance and size, biogenic silica (bSi), particulate organic carbon (POC), and particulate organic nitrogen (PON) cellular content, C/N and Si/C molar ratios of the Rhizaria. Their cellular silicic acid uptake rates (ρ_P) and specific uptake rates (V_P) are also given. Average values were calculated for each zone when possible. For abundances estimates, the mean coefficient of variation (CV) of the triplicates was of 36%, 28%, and 22% for *Protocystis tridens*, *Protocystis harstoni* (Phaeodaria), and Nassellaria, respectively. *n* denotes the number of specimen analyzed.

Station	Subregion	Latitude	Longitude	Species	*n* cells	Abundance (cell m^{-3})	Major axis (μm)	POC (nmol C $cell^{-1}$)	PON (nmol N $cell^{-1}$)	bSi (nmol Si $cell^{-1}$)	C/N	Si/C	ρ_P (nmol Si d^{-1})	V_P (d^{-1})
3	PFZ	−60.564	175.845	*P. tridens*	27	453	101 ± 15	NA	NA	2.3	NA	NA	0.13	0.06
3	PFZ	−60.564	175.845	*P. harstoni*	NA	NA	NA	NA	NA	NA	NA	NA	NA	NA
3	PFZ	−60.564	175.845	Nassellaria	9	51	80 ± 12	NA	NA	4.8	NA	NA	0.56	0.12
5	sACC	−65.877	177.928	*P. tridens*	NA	NA	NA	NA	NA	NA	NA	NA	NA	NA
5	sACC	−65.877	177.928	*P. harstoni*	12	40	101 ± 18	NA	NA	5.8	NA	NA	0.77	0.13
5	sACC	−65.877	177.928	Nassellaria	60	212	74 ± 12	49.3	5.7	2.8	8.7	0.06	0.66	0.24
32	sACC	−65.206	179.247	*P. tridens*	NA	NA	NA	NA	NA	NA	NA	NA	NA	NA
32	sACC	−65.206	179.247	*P. harstoni*	80	8	85 ± 3	34.7	3.8	2.9	9.1	0.08	0.33	0.11
32	sACC	−65.206	179.247	Nassellaria	80	21	101 ± 44	34.2	4.1	1.0	8.3	0.03	0.06	0.06
Mean sACC				Phaeodaria	46	24		34.7	3.8	4.4	9.1	0.08	0.55	0.12
				Nassellaria	70	117		41.7	4.9	1.9	8.5	0.04	0.36	0.15
7	RSR	−70.847	173.924	*P. tridens*	17	16	No picture	NA	NA	4.5	NA	NA	0.97	0.21
7	RSR	−70.847	173.924	*P. harstoni*	17	10	116	NA	NA	7.6	NA	NA	1.32	0.17
7	RSR	−70.847	173.924	Nassellaria	12	41	No picture	NA	NA	4.8	NA	NA	1.00	0.21
9	RSR	−71.499	171.963	*P. tridens*	68	4	96 ± 2	66.5	9.4	0.6	7.1	0.01	0.26	0.42
9	RSR	−71.499	171.963	*P. harstoni*	5	< 1	120	NA	NA	4.7	NA	NA	1.60	0.34
9	RSR	−71.499	171.963	Nassellaria	11	3	81 ± 12	NA	NA	3.6	NA	NA	0.94	0.26
11	RSR	−71.296	177.896	*P. tridens*	58	6	100	100.2	7.8	1.7	12.9	0.02	0.31	0.18
11	RSR	−71.296	177.896	*P. harstoni*	21	2	109 ± 9	106.3	8.3	NA	12.8	NA	NA	NA
11	RSR	−71.296	177.896	Nassellaria	27	1	83 ± 18	NA	NA	3.0	NA	NA	0.80	0.26
13	RSR	−71.694	−176.216	*P. tridens*	51	6	99 ± 12	70.0	7.9	3.0	8.9	0.04	0.82	0.27
13	RSR	−71.694	−176.216	*P. harstoni*	36	5	115 ± 4	139.1	11.3	2.5	12.3	0.02	0.73	0.29
13	RSR	−71.694	−176.216	Nassellaria	75	4	66 ± 5	36.2	3.6	2.8	10.0	0.08	0.58	0.21
15*	RSR	−72.465	−176.333	*P. tridens*	160	2	93 ± 9	42.1	4.5	1.8	9.4	0.04	0.98	0.54
15	RSR	−72.465	−176.333	*P. harstoni*	NA	NA	NA	NA	NA	NA	NA	NA	NA	NA
15	RSR	−72.465	−176.333	Nassellaria	NA	NA	NA	NA	NA	NA	NA	NA	NA	NA
17	RSR	−72.951	−177.655	*P. tridens*	80	3	96 ± 2	23.5	2.3	1.8	10.2	0.08	2.65	1.48

17	RSR	−72.951	−177.655	*P. harstoni*	NA	NA	NA	NA	NA	NA	NA	NA	NA	NA	NA
17	RSR	−72.951	−177.655	Nassellaria	NA	NA	NA	NA	NA	NA	NA	NA	NA	NA	NA
20*	RSR	−73.518	−176.869	*P. tridens*	120	111	93 ± 4	NA	NA	1.7	NA	NA	NA	0.47	0.28
20	RSR	−73.518	−176.869	*P. harstoni*	NA	NA	NA	NA	NA	NA	NA	NA	NA	NA	NA
20	RSR	−73.518	−176.869	Nassellaria	NA	NA	NA	NA	NA	NA	NA	NA	NA	NA	NA
24	RSR	−75.903	−170.558	*P. tridens*	80	11	97 ± 2	33.8	4.5	1.9	7.5	0.06	0.14	0.08
24	RSR	−75.903	−170.558	*P. harstoni*	29	2	111	NA	NA	3.6	NA	NA	1.48	0.41
24	RSR	−75.903	−170.558	Nassellaria	50	6	62 ± 9	NA	NA	3.1	NA	NA	0.19	0.06
26	RSR	−76.415	−166.134	*P. tridens*	NA	NA	NA	NA	NA	NA	NA	NA	NA	NA
26	RSR	−76.415	−166.134	*P. harstoni*	NA	NA	NA	NA	NA	NA	NA	NA	NA	NA
26	RSR	−76.415	−166.134	Nassellaria	46	50	76 ± 8	14.9	1.6	NA	9.3	NA	NA	NA
29	RSR	−68.747	−178.849	*P. tridens*	38	5	89 ± 11	NA	NA	2.3	NA	NA	0.14	0.06
29*	RSR	−68.747	−178.849	*P. harstoni*	42	<1	111 ± 10	NA	NA	2.9	NA	NA	1.59	0.54
29	RSR	−68.747	−178.849	Nassellaria	40	13	92 ± 32	NA	NA	2.3	NA	NA	0.41	0.18
Mean RSR				Phaeodaria	55	14		72.7	7.0	2.9	10.1	0.04	0.96	0.38
				Nassellaria	37	17		25.5	2.6	3.3	9.6	0.08	0.65	0.20

PFZ, Polar Front Zone; RSR, Ross Sea Region; sACC, Southern Antarctic Circumpolar Current.
*The values of organic content are an average value.

Spumellarians were rarely recorded in the samples (fewer than 10 individuals).

Regardless of the taxonomic groups, cell size of the collected specimens varied slightly, ranging from 62 μm for the smallest Nassellaria to a maximum of 115 μm for the largest Phaeodaria (Table 2). Larger cells were rarely recorded in our samples. This is most likely due to the fact that large phaeodarians generally inhabit depth below 200 m (Klaas 2001), where our plankton net tow did not sample.

Overall, biogenic Si per cell varied from 0.6 to 7.6 nmol Si cell^{-1} (Table 2). The POC cellular content varied between 14.9 and 139.1 nmol C cell^{-1}, with the *P. harstoni* being the group with the highest POC content (139.1 nmol C cell^{-1}). The PON cellular content varied between 1.6 and 11.3 nmol N cell^{-1}. Nassellaria had the lowest C/N ratio (9.1 ± 0.7), while Phaeodaria exhibited similar average but more variable C/N ratios (10.0 ± 2.2). The Si/C ratios of Nassellaria (0.05 ± 0.02) and Phaeodaria (0.04 ± 0.03) were similar on average and not significantly different among taxonomic groups (ANOVA, $p = 0.8$). Using cell abundance in the water column and cellular biogenic Si and POC content, we calculated the biogenic Si and POC concentrations of Rhizaria (biogenic Si_{Rhiz} and POC_{Rhiz}) integrated in the upper 200 m of the water column (Fig. 3). Along the latitudinal transect, biogenic Si_{Rhiz} (Fig. 3A) followed the same pattern as cell abundances, with higher values at stations located north of 67°S, in the Polar Front Zone and in the southern Antarctic Circumpolar Current (0.3 and 0.2 mmol Si m^{-2} at Stas. 3 and 5, respectively) although values at Sta. 32 (0.01 mmol Si m^{-2}), located very close to the Sta. 5 were an order of magnitude lower. In the Ross Sea Region, biogenic Si_{Rhiz} concentrations were lower, with an average of 0.02 ± 0.02 mmol Si m^{-2}. Concentrations of POC_{Rhiz} varied from 0.01 to 5.62 mmol C m^{-2} (Fig. 3B). Across the study area, the maximum value of POC_{Rhiz} concentration was observed at Sta. 3, in the Polar Front Zone. In the Ross Sea Region, maximum POC_{Rhiz} concentration (1.28 mmol C m^{-2}) was determined at Sta. 20.

Rhizaria and diatoms silicic acid uptake rate

Silicic acid uptake rate per cell

To our knowledge, this is the first time that silicic acid uptake rates (ρ_P) by Rhizaria were assessed in the Southern Ocean. The measured rates, from 0.58 (± 0.32) nmol Si cell^{-1} d^{-1} for Nassellaria up to 1.12 (± 0.50) nmol Si cell^{-1} d^{-1} for Phaeodaria, were well above than those found for the Mediterranean Sea, which ranged from 0.17 (± 0.05) nmol Si cell^{-1} d^{-1} (Nassellaria) to up to 0.34 ± (0.23) nmol Si cell^{-1} d^{-1} (*Challengeria* spp.—a phaeodarian genus similar to *Protocystis* sp.) (Llopis Monferrer et al. 2020). Silicic acid uptake rates for individual diatoms in the upper 10 m of the water column were estimated using cell abundances obtained through microscopy and the biogenic Si of the sample, as we assume the former was mainly derived from diatoms. In the Ross Sea Region, these values ranged from

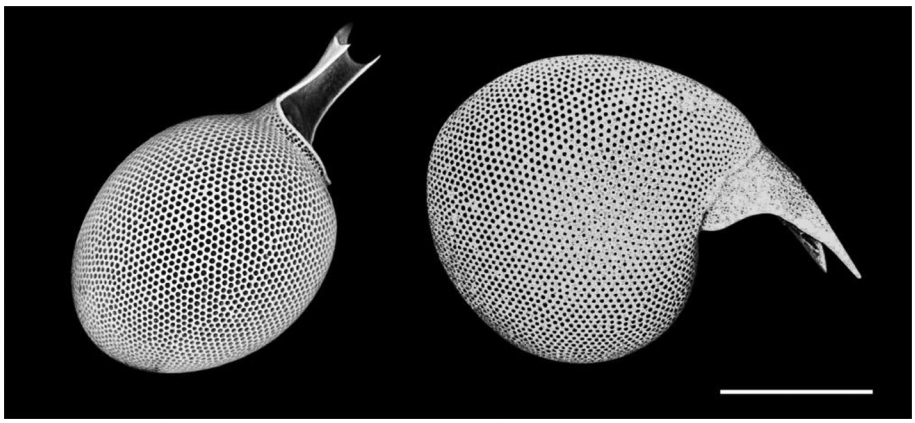

Fig 5. From left to right, scanning electron microscopy (SEM) images of Phaeodaria specimens (*Protocystis tridens* and *Protocystis harstoni*). Scale bar = 50 μm.

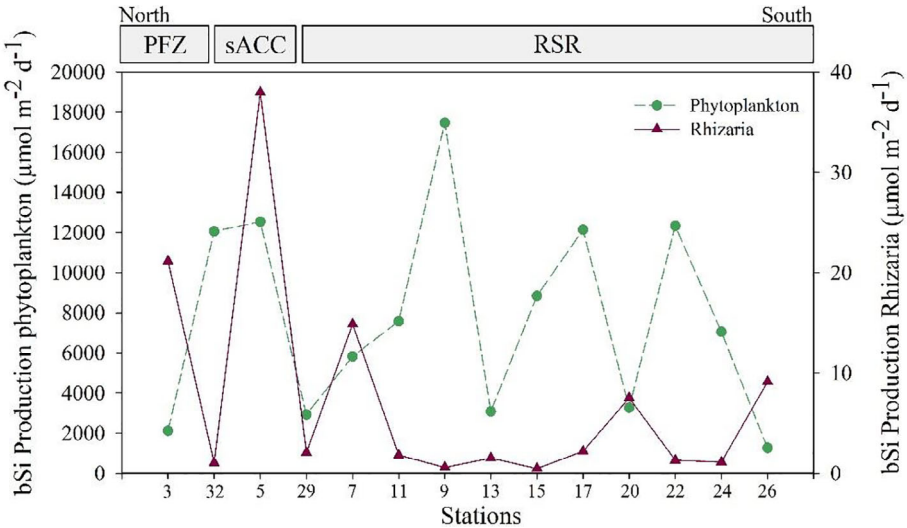

Fig 6. Water column integrated biogenic silica (bSi) production for the phytoplankton community (diatoms) and Rhizaria, respectively (100 m for phytoplankton community and 200 m for rhizarians due to the net tow extension). Polar Front Zone (PFZ), southern Antarctic Circumpolar Current (sACC) and Ross Sea Region (RSR). *Y*-axis for phytoplankton and Rhizaria vary by several orders of magnitude.

0.9 to 18.5 pmol Si cell^{-1} d^{-1} with an average of 8.3 (± 6.6) pmol Si cell^{-1} d^{-1}.

Specific silica uptake rates

Specific Si uptake rates (V_P—silicic acid uptake rates normalized to biogenic Si concentrations) of the phytoplankton community were on average 0.06 d^{-1} (range < 0.01–0.12) at 10 m depth (Table 1). These rates tended to be higher in the Ross Sea Region (average 0.08 d^{-1}) compared to those measured in the southern Antarctic Circumpolar Current (average 0.03 d^{-1}) and Polar Front Zone (average 0.01 d^{-1}). Specific Si uptake rates for Rhizaria were higher than those found for the phytoplankton community, averaging 0.18, 0.36 and 0.29 d^{-1} for Nassellaria, *P. tridens* and *P. harstoni*, respectively (Table 2), which are in line with values measured in the Mediterranean Sea (0.07–0.48 d^{-1}) (Llopis Monferrer et al. 2020). These values are also consistent with specific growth rates of the Aulosphaeridae (large Phaeodaria) estimated from theoretical values, which were in the range of 0.05 and 0.5 d^{-1} (Stukel et al. 2018). Comparing to phytoplankton, specific Si uptake rates for Rhizaria are close to those previously reported for Antarctic diatoms (0.31 d^{-1}) (Nelson et al. 2001), and also from diatoms found in other warmer oceanic regions (0.19 d^{-1}) (Leblanc et al. 2003). Siliceous phytoplankton-specific Si uptake rates in the Ross Sea Region (Fig. 1) were, on average, 0.08 ± 0.03 d^{-1}, in accordance to what has been previously found in this region (0.06 d^{-1}) by Nelson and Tréguer (1992). These values are much lower than those in other more productive oceanic regions such as the Peru upwelling (1.8 d^{-1}, Goering et al. 1973) or California (1.02 d^{-1}, White and Dugdale 1997).

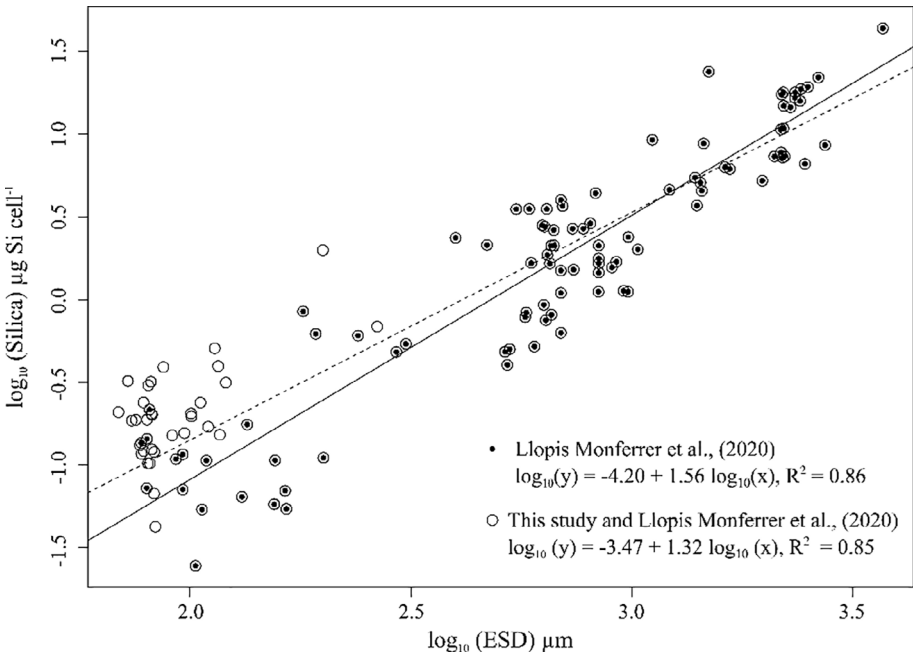

Fig 7. Relationship between the Si content of Polycystina and Phaeodaria and their equivalent spherical diameter (ESD, μm) across all the specimens assessed. Black dots represent data from Llopis Monferrer et al. (2020), which include data from Biard et al. (2018). White dots are all data including that of this study. Linear regression (solid line) of the Llopis Monferrer et al. (2020) data and linear regression (dashed line) for the combination of data from this study and Llopis Monferrer et al. (2020).

Biogenic silica production rates integrated in the water column

Rates of silicic acid uptake (ρ_P) integrated in the upper water column ranged from 1264.0 to 17,474.2 μmol Si m^{-2} d^{-1} for diatoms and from 0.48 to 37.97 μmol Si m^{-2} d^{-1} for Rhizaria, respectively (Fig. 6). Phytoplankton community rates of silicic acid uptake were always two or three orders of magnitude higher than Rhizaria silicic acid uptake rates. At Sta. 5, located in the Southern Antarctic Circumpolar Current, some of the highest production values for both, diatoms (12,541.4 μmol Si m^{-2} d^{-1}) and Rhizaria (38.0 μmol Si m^{-2} d^{-1}), were found. The northern stations generally displayed the highest Rhizaria silicic acid uptake rates values found during the expedition (Stas. 3, 5, and 7 with 21.2, 38.0, and 14.9 μmol Si m^{-2} d^{-1}, respectively). In the Ross Sea Region, we found the highest values of silicic acid uptake rates for phytoplankton community (17,474.2 μmol Si m^{-2} d^{-1}) at coastal Sta. 9 off Cape Adare.

Discussion

Are Rhizaria more silicified in the Southern Ocean?

Allometric relationship for Rhizaria

The biogenic Si content of siliceous Rhizaria has been investigated using different approaches, from living cells collected with net-tows (Biard et al. 2018; Llopis Monferrer et al. 2020), and settling cells recovered from sediment traps (Takahashi 1981), to fossil assemblages from the sediments (Lazarus et al. 2009). An allometric relationship was established by Biard et al. (2018) showing a good correspondence between Si content and biovolume of large Rhizaria (Phaeodaria; > 600 μm). This relationship was expanded by Llopis Monferrer et al. (2020) over a wider size range (from 78 to 3698 μm). When adding the information on silica content of the samples collected in the present survey to the former relationship, the silica content remains significantly correlated with the cell's equivalent spherical diameter (ESD; R^2 = 0.85, p < 0.001, n = 126) (Fig. 7) according to the following equation:

$$\log_{10}\left(Q_{\text{biogenic Si}}\right) = [-3.47 \pm 0.13] + [1.32 \pm 0.05]\log_{10}(\text{ESD}),$$

where $Q_{\text{biogenic Si}}$ is the silica content in μg Si cell^{-1}. When plotting silica content versus ESD for our data set alone, the slope is significantly different (ANCOVA, p < 0.01) from the one calculated by Llopis Monferrer et al. (2020). Specimens analyzed for the present study display higher silica content than specimen of similar size found in other areas of the global ocean (Fig. 7), suggesting a higher degree of silicification of rhizarians in the silicic acid-rich Southern Ocean.

Note that if the amount of silica per cell is high, so is the cell's capacity to take up silicic acid. Indeed, the biogenic Si production by Rhizaria per cell is up to three orders of magnitude higher than that found for diatoms. The one order of magnitude larger size of rhizarians than diatoms might

explain in part, the difference. Rhizaria are heavily silicified organisms; however, their Si/C ratio in this study (0.05 ± 0.03) is rather low when compared to those found for the phytoplankton community (mainly diatoms) (0.21 ± 0.13), or to the reference value 0.13 for diatoms growing in replete nutrients conditions (Brzezinski 1985). The Si/C ratio found for Rhizaria in the Southern Ocean is close to that found in the Mediterranean Sea (Llopis Monferrer et al. 2020), which indicates some steadiness despite contrasting environmental conditions. Caution should be taken because of the limited data set, but at present, there is no evidence of an increase in the Si/C ratio for rhizarians in the Southern Ocean. Such increase is often seen in diatoms (Smith and Kaufman 2018), in response to high silicic acid concentrations found at high latitudes, or to micronutrient limitation, particularly iron (Leynaert et al. 2004; Claquin et al. 2006).

Previous data of C/N molar ratios for Rhizaria are scarce. In the samples collected during the TAN1901 expedition, the C/N ratio was 9.7 on average (7.1–12.9), higher than the Redfield ratio (6.6), but similar to those found by Michaels et al. (1995) for colonial radiolarians (8.2) and by Llopis Monferrer et al. (2020) for several rhizarian groups including Nassellaria, Spumellaria, Collodaria, and Phaeodaria (average 12). The C/N ratios of the phytoplankton of the TAN1901 expedition were within the range observed for actively growing phytoplankton assemblages and cultures (6.3 ± 1.4) (Garcia et al. 2018). In contrast, the C/N ratios observed in the present study for phytoplankton were highly variable in comparison with previous studies (Michaels et al. 1995; Llopis Monferrer et al. 2020), which conflicts with their consistent Si/C from different regions. This suggests that C/N ratios are affected by species compositions and/or environmental conditions. Moreover, a substantial fraction of Polycystine radiolarians harbor symbionts (Decelle et al. 2015), which may also influence the C/N ratios. During the TAN1901, some individuals appeared to be feeding on diatoms, very abundant in the study area, suggesting that the predation could also affect the molar ratios. Further investigations should be made to explore to which extent this photosymbiotic association and predation may affect molar ratios.

Distribution and biogenic silica production of small Rhizaria in the surface of the Southern Ocean

Rhizaria abundances

The general trend in distribution and abundances of Rhizaria observed during the TAN1901 expedition is similar to data reported in other sectors of the Southern Ocean (Abelmann and Gowing 1997), with higher values as we go northward (Table 3). However, they contrast with the findings by Klaas (2001) in the Weddell Sea during October–November 1992, where highest abundances of rhizarians were observed at lower latitudes and abundances were overall much higher than those found in the present study. This may reflect seasonal, geographic or species differences in the Rhizaria community sampled. Other factors, such as temperature, salinity, and chlorophyll can control the community structure and abundance of rhizarians. Hu et al. (2015), for example, showed a link between highest abundance and the deep Chl *a* maximum in the South China Sea. They also highlighted the co-influence of temperature when the maximum abundance appeared in the top 25 m of the water column in cold eddies.

During the TAN1901 expedition, we observed a sharp variation in cell abundances within the Southern Antarctic Circumpolar Current, between Stas. 5 and 32, which were very

Table 3. Mean abundances or ranges (in parentheses) of polycystine radiolarians and Phaeodaria in polar waters found in this study and reported in previous surveys.

Reference	Area	Season	Year	Depth interval (m)	Polycystina (cells m^{-3})	Phaeodaria (cells m^{-3})
This study	Ross Sea—PFZ	Jan–Feb	2019	0–200	51	453
	Ross Sea—sACC	Jan–Feb	2019	0–200	(21–212)	(8–40)
	Ross Sea—RSR	Jan–Feb	2019	0–200	(1–41)	(< 1–111)
Llopis Monferrer et al. (2020)	> 40°N–S	NA	2020	0–200	182	5
Abelmann and Gowing (1997)	> 45°S (Atlantic sector)	April	1991	0–200	(325–408)	NA
	< 45°S (Atlantic sector)	April	1991	0–200	(31–583)	NA
Alder and Boltovskoy (1993)	Weddell Sea	March	1991	0–200	NA	700
	Weddell Sea	Nov–Jan	1986	0–200	1441	534
Klaas (2001)	Weddell Sea—PFZ	Oct–Nov	2001	0–200	(5464–6595)	(1750–3952)
	Weddell Sea—sACC	Oct–Nov	2001	0–200	(332–336)	(125–521)
	Weddell Sea—AWB	Oct–Nov	2001	0–200	(627–1413)	(218–852)
Morley and Stepien (1985)	Weddell Sea	Oct–Nov	1981	0–200	(22–176)	(32–155)
Tanaka and Takahashi (2008)	Subarctic Pacific	June	2006	0–250	NA	6

AWB, Antarctic Circumpolar Current–Weddell Gyre Boundary; PFZ, Polar Front Zone; RSR, Ross Sea Region; sACC, southern Antarctic Circumpolar Current.

closely located. The Antarctic Circumpolar Current is a known area for high kinetic energy dissipation that can generate a large spatial heterogeneity at sub-mesoscale and affect plankton distribution (Carrasco et al. 2003), including that of Rhizaria. This dynamic area produces large variations in temperature which can affect living Rhizaria, and therefore their ecological distributions (Hu et al. 2015). The differences observed could also be explained by the delay of the sampling date as Sta. 5 was sampled on the outward journey, 25 days before Sta. 32 which was sampled on the return leg, corresponding potentially to a different period of the development of Rhizaria communities, for which information is still lacking. Linking the variability observed between short-term abundances data to the seasonal dynamic of these protists or to rapid changes in environmental conditions is still a challenge. No global relationship between Rhizaria abundances and biotic or abiotic parameters was found during TAN1901. This study illustrates the difficulty in the interpretation of data from campaigns where sampling is limited in time and space.

Rhizaria biogenic silica production in the Southern Ocean

This is the first time that the silicic acid uptake rates of rhizarians were measured directly in the Southern Ocean. Previous global measurements of silicic acid uptake rates by these were obtained indirectly, from worldwide Rhizaria abundances and converted into biogenic Si production, using single cell uptake rates from the Mediterranean Sea's specimens (Llopis Monferrer et al. 2020). They estimated that Rhizaria may produce, in polar waters (> 40°N–S), between 0.4 and 6.4 Tmol Si yr^{-1}, that is, about 10% of the world biogenic Si production by rhizarians, which was estimated to be between 5 and 58 Tmol Si yr^{-1}. Their estimate for the surface layer of the polar waters was between 0.1 and 53.8 μmol Si m^{-2} d^{-1}, which matches with the direct measurements made during this study (0.8–36.8 μmol Si m^{-2} d^{-1}, Table 4).

Table 4. Biogenic silica stocks (bSi) and silicic acid uptake rates (ρ_P) integrated in the upper water column for diatoms and Rhizaria, respectively.

		bSi (mmol Si m^{-2})		ρ_P (μmol Si m^{-2} d^{-1})	
Station #	Subregion	Rhizaria	Diatoms	Rhizaria	Diatoms
3	PFZ	0.27	284	21.1	2119
32	sACC	0.01	348	1.2	12,062
5	sACC	0.17	280	36.8	12,541
Mean sACC		0.09	314	19.0	12,302
29	RSR	0.01	32	1.7	2927
7	RSR	0.07	118	13.6	5828
11	RSR	0.00	134	2.2	7572
9	RSR	0.00	276	0.8	17,474
13	RSR	0.01	67	2.1	3085
15	RSR	0.00	110	0.3	8842
17	RSR	0.00	177	2.4	12,139
20	RSR	0.04	73	7.5	3269
22	RSR	0.00	150	1.3	12,330
24	RSR	0.01	78	1.1	7056
26	RSR	0.04	24	9.2	1264
Mean RSR		0.02	113	3.8	7435

PFZ, Polar Front Zone (PFZ); RSR, Ross Sea Region; sACC, southern Antarctic Circumpolar Current.

An Antarctic paradox for siliceous Rhizaria?

Given the high silicic acid concentration, the Antarctic Ocean is expected to favor the production of pelagic silicifiers, including Rhizaria. During the TAN1901 expedition, silicic acid uptake rates of Rhizaria were measured in parallel to those of diatoms. The silicic acid uptake rates of Rhizaria measured were very low when compared to those of diatoms. Indeed, when comparing the averages measured in each zone, rhizarians would only represent 0.05% in the Ross Sea Region, 0.15% in the Southern Antarctic Circumpolar Current, and 1% in the Polar Front Zone of the diatoms biogenic Si production (Table 4).

From data acquired during the *Tara* Ocean circum-expedition, Hendry et al. (2018) suggested that diatoms might exclude Rhizaria because they display a strong affinity for silicic acid and thus outcompete Rhizaria in the photic zone and shallow depths where silicic acid is often scarce. However, high abundances of Phaeodaria have been associated with high primary production and diatom blooms, some of them being from high-latitude areas where silicic acid is rarely limiting (Nimmergut and Abelmann 2002; Dolan et al. 2014). Little is known about which factors regulate the abundance and silicic acid uptake rates by rhizarians. Moreover, our data did not show any reliable statistical relationship with either silicic acid or with Chl *a* concentration. Thus, this concept of an exclusive relationship between diatom and Rhizaria abundances does not seem to be universal. In the sediments of areas around Antarctica, it has been reported that some biogenic oozes can be dominated by radiolarians (Dutkiewicz et al. 2015). Analysis of a sediment core in the Pacific region of the Southern Ocean showed that most of the sedimentary biogenic Si was represented by diatoms, but radiolarians could contribute up to 6% of the total biogenic Si (Maldonado et al. 2019). It becomes a paradox that with less than 1% contribution to biogenic Si production in the 0–200-m water layer, Rhizaria can make a very substantial contribution to biogenic Si burial in the deep ocean. Following we will try to provide some explanations to this paradox.

Firstly, we contemplate a large underestimation of Rhizaria production by our sampling strategy. While diatoms are photosynthetic organisms that thrive in the photic zone, Rhizaria inhabit the entire water column (Biard and Ohman 2020), with specific communities and highest abundances occurring at depth (peak at 200–400 m in southern latitudes; Suzuki and Not 2015). Although they present low cell densities, deep-

living species usually inhabit much larger depth intervals, and cell abundance integration results in high standing stocks comparable to those estimated for surface communities (Kling and Boltovskoy, 1995). Other studies highlight the importance of Rhizaria in the twilight zone, with approximately 50% of the phaeodarians inhabiting between 250 and 3000 m depth (Tanaka and Takahashi 2008). Since our plankton tows did not extend below 200 m, groups of deep-living Rhizaria were not considered in our global Si budget. According to Llopis Monferrer et al. (2020), between 62% and 75% of the biomass and Si production of the Rhizaria occurring at high latitudes (> 40°N–S) would take place in the twilight zone, below 200 m depth. Thus, the production measured in this study would account for no more than half of the Rhizaria production that takes place in the entire water column.

Second, we should take into account seasonality. While the overall pattern of phytoplankton evolution is well studied in this area, with a spring bloom of haptophyte that accumulates until late December, followed by a diatoms bloom (Smith and Kaufman 2018), little information is available about rhizarians dynamics. Plankton-tow samples provide limited coverage in space and time for estimating standing stocks. Extrapolation of cell densities from this study to year-round budgets could be biased by the seasonality of Rhizaria communities. Boltovskoy et al. (1993) found that radiolarians abundances (as recorded in sediment trap samples that integrate the signal over longer time scales) can vary throughout the year over one order of magnitude. This poses the possibility that our samples overestimated the Rhizaria densities. To clearly understand the influence of environmental factors on Rhizaria seasonality and distribution patterns in this complex and dynamic region, further studies with a better temporal coverage are needed as well as performing a more specific taxonomic classification (e.g., reaching species level) (Abelmann and Gowing 1997) are required.

Eventually, the rate of dissolution between Rhizaria and diatoms is different (Maldonado et al. 2019). Some forms of Rhizaria skeleton, and especially the polycystine radiolarians (Takahashi 1981), are much more resistant than diatoms' frustules. Moreover, Rhizaria remineralization occurs mostly on the sea-floor (Takahashi 1981), while diatoms dissolution occurs both in the water column and in the sediments (Tréguer and De La Rocha 2013; Tréguer et al. 2021). These two processes combined, would lead to a preferential preservation of the Rhizaria at the sediment surface. Despite the lower abundance of Rhizaria relative to diatoms in the euphotic layer of the Southern Ocean, their presence throughout the entire water column, their overall higher resistance to dissolution, and the high individual silicic acid uptake rates measured in this study confer them a potentially important role on the Si cycling and export to the deep ocean. This study highlights the need of rhizarians studies in the twilight zone, where these protists may be the sole pelagic silicic acid consumers. Future research on the global significance of Rhizaria relatively to diatoms in the silicon biogeochemical cycle requires the study of the factors controlling the former distributions considering a holistic approach of the entire Rhizaria size range.

References

Abelmann, A., and M. M. Gowing. 1997. Spatial distribution pattern of living polycystine radiolarian taxa—Baseline study for paleoenvironmental reconstructions in the Southern Ocean (Atlantic sector). Mar. Micropaleontol. **30**: 3–28. doi:10.1016/S0377-8398(96)00021-7

Alder, V. A., and D. Boltovskoy. 1993. The ecology of larger microzooplankton in the Weddell-Scotia Confluence Area: Horizontal and vertical distribution patterns. **51**: 323–344. doi:10.1357/0022240933223783

Biard, T., J. W. Krause, M. R. Stukel, and M. D. Ohman. 2018. the significance of giant phaeodarians (Rhizaria) to biogenic silica export in the California current ecosystem. Global Biogeochem. Cycl. **32**: 987–1004. doi:10.1029/2018GB005877

Biard, T., and M. D. Ohman. 2020. Vertical niche definition of test-bearing protists (Rhizaria) into the twilight zone revealed by in situ imaging. Limnol. Oceanogr. **65**(11): 2583–2602. doi:10.1002/lno.11472

Boltovskoy, D., V. A. Alder, and A. Abelmann. 1993. Annual flux of radiolaria and other shelled plankters in the eastern equatorial atlantic at 853 m: Seasonal variations and polycystine species-specific responses. Deep Sea Res. Part I Oceanogr. Res. Pap. **40**: 1863–1895. doi:10.1016/0967-0637(93)90036-3

Brzezinski, M. A. 1985. The Si:C:N ratio of marine diatoms: Interspecific variability and the effect of some environmental variables. J. Phycol. **21**: 347–357.

Brzezinski, M. A., and D. M. Nelson. 1989. Seasonal changes in the silicon cycle within a Gulf Stream warm-core ring. Deep Sea Res. Part A. Oceanog. Res. Pap. **36**: 1009–1030. doi:10.1016/0198-0149(89)90075-7

Brzezinski, M. A., and D. R. Phillips. 1997. Evaluation of ^{32}Si as a tracer for measuring silica production rates in marine waters. Limnol. Oceanogr. **42**: 856–865. doi:10.4319/lo.1997.42.5.0856

Carrasco, J. F., D. H. Bromwich, and A. J. Monaghan. 2003. Distribution and characteristics of mesoscale cyclones in the Antarctic: Ross Sea Eastward to the Weddell Sea. Mon. Weather Rev. **131**: 13.

Claquin, P., A. Leynaert, A. Sferratore, J. Garnier, and O. Ragueneau. 2006. Physiological ecology of diatoms along the river-sea continuum, p. 121–138.*In* The silicon cycle. Human perturbations and impacts on aquatic systems. Island Press.

Decelle, J., S. Colin, and R. A. Foster. 2015. Photosymbiosis in marine planktonic protists, p. 465–500.*In* Marine protists. Springer.

Dolan, J. R., E. J. Yang, T. W. Kim, and S.-H. Kang. 2014. Microzooplankton in a warming Arctic: A comparison of tintinnids and radiolarians from summer 2011 and 2012 in the Chukchi Sea. **14**.

Dutkiewicz, A., R. D. Müller, S. O'Callaghan, and H. Jónasson. 2015. Census of seafloor sediments in the world's ocean. Geology **43**: 795–798. doi:10.1130/G36883.1

Garcia, N. S., J. Sexton, T. Riggins, J. Brown, M. W. Lomas, and A. C. Martiny. 2018. High variability in cellular stoichiometry of carbon, nitrogen, and phosphorus within classes of marine eukaryotic phytoplankton under sufficient nutrient conditions. Front. Microbiol. **9**: 543. doi:10.3389/fmicb.2018.00543

Goering, J. J., D. M. Nelson, and J. A. Carter. 1973. Silicic acid uptake by natural populations of marine phytoplankton. Deep Sea Res. Oceanogr. Abst. **20**: 777–789. doi:10.1016/0011-7471(73)90001-6

Hendry, K. R., A. O. Marron, F. Vincent, D. J. Conley, M. Gehlen, F. M. Ibarbalz, B. Quéguiner, and C. Bowler. 2018. Competition between silicifiers and non-silicifiers in the past and present ocean and its evolutionary impacts. Front. Mar. Sci. **5**: 22. doi:10.3389/fmars.2018.00022

Honjo, S., S. J. Manganini, R. A. Krishfield, and R. Francois. 2008. Particulate organic carbon fluxes to the ocean interior and factors controlling the biological pump: A synthesis of global sediment trap programs since 1983. Prog. Oceanogr. **76**: 217–285. doi:10.1016/j.pocean.2007.11.003

Hu, W., L. Zhang, M. Chen, L. Zeng, W. Zhou, R. Xiang, Q. Zhang, and S. Liu. 2015. Distribution of living radiolarians in spring in the South China Sea and its responses to environmental factors. Sci. China Earth Sci. **58**: 270–285. doi:10.1007/s11430-014-4950-0

Klaas, C. 2001. Spring distribution of larger (> 64 μm) protozoans in the Atlantic sector of the Southern Ocean. Deep Sea Res. Part I **48**: 1627–1649.

Kling, S. A., and D. Boltovskoy. 1995. Radiolarian vertical distribution patterns across the Southern California current. Deep Sea Research Part I: Oceanographic Research Papers **42**: 191–231. doi:10.1016/0967-0637(94)00038-T

Latasa, M. 2014. A simple method to increase sensitivity for RP-HPLC phytoplankton pigment analysis: Increased HPLC sensitivity. Limnol. Oceanogr. Methods **12**: 46–53. doi:10.4319/lom.2014.12.46

Lazarus, D. B., B. Kotrc, G. Wulf, and D. N. Schmidt. 2009. Radiolarians decreased silicification as an evolutionary response to reduced Cenozoic ocean silica availability. Proc. Natl. Acad. Sci. **106**: 9333–9338. doi:10.1073/pnas.0812979106

Leblanc, K., B. Quéguiner, N. Garcia, P. Rimmelin, and P. Raimbault. 2003. Silicon cycle in the NW Mediterranean Sea: seasonal study of a coastal oligotrophic site. Oceanol. Acta **26**: 339–355. doi:10.1016/S0399-1784(03)00035-5

Leynaert, A., P. Tréguer, D. M. Nelson, and Y. Del Amo. 1996. 32 Si as a tracer of biogenic silica production: methodological improvements, p. 29–35. *In* Integrated marine system analysis. Vrije Universiteit Brussel.

Leynaert, A., E. Bucciarelli, P. Claquin, R. C. Dugdale, V. Martin-Jézéquel, P. Pondaven, and O. Ragueneau. 2004. Effect of iron deficiency on diatom cell size and silicic acid uptake kinetics. Limnol. Oceanogr. **49**: 1134–1143. doi:10.4319/lo.2004.49.4.1134

Llopis Monferrer, N., D. Boltovskoy, P. Tréguer, M. M. Sandin, F. Not, and A. Leynaert. 2020. Estimating biogenic silica production of Rhizaria in the global ocean. Global Biogeochem. Cycles **34**(3). doi:10.1029/2019GB006286

Maldonado, M., M. López-Acosta, C. Sitjà, M. García-Puig, C. Galobart, G. Ercilla, and A. Leynaert. 2019. Sponge skeletons as an important sink of silicon in the global oceans. Nat. Geosci. **12**: 815–822. doi:10.1038/s41561-019-0430-7

Michaels, A. F., D. A. Caron, N. R. Swanberg, F. A. Howse, and C. M. Michaels. 1995. Planktonic sarcodines (Acantharia, Radiolaria, Foraminifera) in surface waters near Bermuda: Abundance, biomass and vertical flux. J. Plankton Res. **17**: 131–163. doi:10.1093/plankt/17.1.131

Morley, J. J., and J. C. Stepien. 1985. Antarctic Radiolaria in Late Winter/Early Spring Weddell Sea Waters. Micropaleontology **31**: 365. doi:10.2307/1485593

Nelson, D. M., and L. I. Gordon. 1982. Production and pelagic dissolution of biogenic silica in the Southern Ocean. Geochim. Cosmochim. Acta **46**: 491–501. doi:10.1016/0016-7037(82)90153-3

Nelson, D. M., and P. Tréguer. 1992. Role of silicon as a limiting nutrient to Antarctic diatoms: evidence from kinetic studies in the Ross Sea ice-edge zone. Mar. Ecol. Prog. Ser. **80**: 255–264.

Nelson, D. M., M. A. Brzezinski, D. E. Sigmon, and V. M. Franck. 2001. A seasonal progression of Si limitation in the Pacific sector of the Southern Ocean. Deep-Sea Res. II Top. Stud. Oceanogr. **48**: 3973–3995. doi:10.1016/S0967-0645(01)00076-5

Nimmergut, A., and A. Abelmann. 2002. Spatial and seasonal changes of radiolarian standing stocks in the Sea of Okhotsk. Deep-Sea Res. I Oceanogr. Res. Pap. **49**: 463–493. doi:10.1016/S0967-0637(01)00074-7

Nöthig, E.-M., and M. M. Gowing. 1991. Late winter abundance and distribution of phaeodarian radiolarians, other large protozooplankton and copepod nauplii in the Weddell Sea. Antarctica. Mar. Biol. **111**: 473–484. doi:10.1007/BF01319421

Olenina, I., S. Hadju, L. Edler, and others. 2006. Biovolumes and size-classes of phytoplankton in the Baltic Sea. Helsinki Commision, Baltic Marine Environment Protection Commission.

Ragueneau, O., and P. Tréguer. 1994. Determination of biogenic silica in coastal waters: Applicability and limits of the alkaline digestion method. Mar. Chem. **45**: 43–51. doi:10.1016/0304-4203(94)90090-6

Safi, K. A., F. Brian Griffiths, and J. A. Hall. 2007. Microzooplankton composition, biomass and grazing rates along the WOCE SR3 line between Tasmania and Antarctica. Deep-Sea Res. I Oceanogr. Res. Pap. **54**: 1025–1041. doi:10.1016/j.dsr.2007.05.003

Smith, W. O., and D. E. Kaufman. 2018. Climatological temporal and spatial distributions of nutrients and particulate matter in the Ross Sea. Progress in Oceanography **168**: 182–195. doi:10.1016/j.pocean.2018.10.003

Stukel, M. R., T. Biard, J. Krause, and M. D. Ohman. 2018. Large Phaeodaria in the twilight zone: Their role in the carbon cycle: Phaeodarian ecology in the twilight zone. Limnol. Oceanogr. **63**: 2579–2594. doi:10.1002/lno.10961

Sun, J., and D. Liu. 2003. Geometric models for calculating cell biovolume and surface area for phytoplankton. J. Plankton Res. **25**: 1331–1346. doi:10.1093/plankt/fbg096

Suzuki, N., and F. Not. 2015. Biology and ecology of radiolaria, p. 179–222.*In* Marine protists: Diversity and dynamics. Springer.

Takahashi, K. 1981. Vertical flux, ecology and dissolution of radiolaria in tropical oceans: Implications for the silica cycle.

Tanaka, S., and K. Takahashi. 2008. Detailed vertical distribution of radiolarian assemblage (0–3000 m, fifteen layers) in the central subarctic Pacific, June 24, 2006.

Tréguer, P., L. Lindner, A. J. van Bennekom, A. Leynaert, M. Panouse, and G. Jacques. 1991. Production of biogenic silica in the Weddell-Scotia Seas measured with ^{32}Si. Limnol. Oceanogr. **36**: 1217–1227. doi:10.4319/lo.1991.36.6.1217

Tréguer, P., D. M. Nelson, A. J. Van Bennekom, D. J. DeMaster, A. Leynaert, and B. Queguiner. 1995. the silica balance in the world ocean: A reestimate. Science **268**: 375–379. doi:10.1126/science.268.5209.375

Tréguer, P., and C. L. De La Rocha. 2013. The world ocean silica cycle. Annu. Rev. Mar. Sci. **5**: 477–501. doi:10.1146/annurev-marine-121211-172346

Tréguer, P. J. 2014. The southern ocean silica cycle. Compt. Rendus Geosci. **346**: 279–286. doi:10.1016/j.crte.2014.07.003

Tréguer, P. J., and others. 2021. Reviews and syntheses: The biogeochemical cycle of silicon in the modern ocean. Biogeosciences, **18**: 1269–1289.

Uitz, J., H. Claustre, A. Morel, and S. B. Hooker. 2006. Vertical distribution of phytoplankton communities in open ocean: An assessment based on surface chlorophyll. J. Geophys. Res. **111**: C08005. doi:10.1029/2005JC003207

Utermöhl, H. 1958. Zur Ver vollkommung der quantitativen phytoplankton-methodik. Mitt. Int. Verein. Theor. Amgew. Limnol. **9**: 1–38.

White, K. K., and R. C. Dugdale. 1997. Silicate and nitrate uptake in the Monterey Bay upwelling system. Cont. Shelf Res. **17**: 455–472. doi:10.1016/S0278-4343(96)00042-8

Acknowledgments

The authors would like to thank the captain and crew of R.V. Tangaroa for their efforts in facilitating the sampling during TAN1901, as well as other participants for their help. We thank H. Whitby, N. van Horsten, M. López-Acosta, and Wen-Hsuan Liao for their valuable help. We are particularly grateful to D. Boltovskoy and E. Thiébaut for their helpful comments and fruitful discussions. We also would like to thank M. Legoff for the silicic acid analysis. This work was funded in New Zealand by MBIE Endeavour Fund programme Ross-RAMP (C01X1710) with assistance from NIWA Strategic Science Investment Fund (SIFF) Coasts and Oceans, Programme 4. This work was supported by the French National program LEFE (Les Enveloppes Fluides et l'Environnement) and ANR RadiCal (ANR-18-CE01-0011). We thank the anonymous reviewers for constructive comments.

Conflict of Interest

None declared.

Submitted 24 July 2020
Revised 06 December 2020
Accepted 21 February 2021

Associate editor: Bo Thamdrup